Finite Element Analysis of Molecular Rydberg States

M. G. Levy, R. M. Stratt, and P. M. Weber*
Brown University Department of Chemistry
*Corresponding author: Box H, 324 Brook Street, Providence RI 02912, Peter_Weber@brown.edu

Abstract: Identifying molecules requires associating molecular structures with their electronic energy levels. In this paper we introduce a novel technique for the calculation of molecular Rydberg levels. The technique allows for easy visualization of the associated wavefuntions to make unambiguous assignments. The value calculated for the 3p state of *trimethylamine* is most closely in agreement with recent experimental data. The 3s state was also calculated. The method, which should be extendable to all Rydberg-excited molecules, appears to increase in accuracy for higher-lying states.

Keywords: Rydberg States, Molecular Physics, Computational Chemistry, Quantum Mechanics

1. Introduction

In quantum mechanics there are very few analytically solvable problems. One of the more famous ones is the Hydrogen Atom. In this study we liken more complicated molecules, like trimethylamine, to the hydrogen case, noting that these many-electron-containing molecules can be excited into a regime where there is a single electron acting as if it were orbiting around a molecular core with a frozen charge distribution. Such highly excited states are known as Rydberg states.[1] We calculate the electron binding energies associated with the Rydberg states of different molecules using quantum chemical *ab initio* calculations to compute the core charge distribution and compare our computational spectra with experimentally measured eigenvalues. We also discuss aspects of using and importing the results from such calculations into COMSOL.

2. Governing Equation

Electronic behavior is governed by a PDE known as the Schrödinger equation:

$$-\frac{\hbar^2}{2m}\nabla^2 u + Vu = \lambda u$$

with Drichlet boundary condition u = 0 at ∞. $\hbar$ and m are constants. u is referred to as the wavefunction. In quantum mechanics, u^2 is the probability density of finding the particle at $\mathbf{r}$ and as such,

$$\int u^2 d\mathbf{r} = 1.$$

V is a potential energy, which in our treatment depends on the frozen core charge density ρ.

$$V = e^2 \int \frac{d\mathbf{r}'}{|\mathbf{r} - \mathbf{r}'|} \rho(\mathbf{r}; \mathbf{R}_N)$$

$$\mathbf{R}_N = \{\mathbf{r}_1, ..., \mathbf{r}_N\},$$

where $\mathbf{R}_N$ represents the nuclear positions, and e is the unit charge. λ is the energy eigenvalue we are solving for.

3. Theory

We are approximating this many-electron problem as a combination of an excited-state single electron problem and a separate ground-state multi-electron problem. It is much easier to solve for the electric potential induced by the ground state of the molecular core than it would be to calculate the desired high lying eigenvalues of the whole molecule using Hartree-Fock or DFT self-consistent field based methods. Thus we use standard computational chemistry techniques to calculate the former and then import the resultant potential into COMSOL to provide us with the later. One can think of our problem as analogous to a particle in an external field, the field defined by the three-dimensional, not necessarily symmetric, result from the computational chemistry calculation.

The justification for this analysis is that Rydberg states have a single electron excited into a distant regime from where the molecular core looks much like a point charge. At large distance there is little correlation between the bound electrons and the Rydberg-excited electron. In practice that means that the root mean square distance of the Rydberg electron from the center of charge $\bar{\mathbf{r}}$

$$\sqrt{\langle r^2 \rangle} = \int (\mathbf{r} - \bar{\mathbf{r}})^2 u^2 d\mathbf{r}$$

must be of the order of or greater than the size of the molecular core. Our calculations can be seen as both a test of this approximation and as probing the viability of the electronic potential computed by Gaussian's PRISIM algorithm.[2]

4. Methodology

We chose to work within standard atomic units as the system sets $\hbar$, m, and e to 1. In this system the bohr (0.529×10^{-10} m) is the length unit, and our Drichlet boundary, forming a spherical box, set to 50 bohr. V, defined as an imported interpolated function over a three dimensional spatial grid, was derived from a DFT calculation run in GAUSSIAN 03[3] on the cationic state after parsing the data using the GAUSSIAN routine cubegen and some self-written MATLAB[4] scripts. Once the model was defined using the COMSOL GUI we utilized the PARDISO linear solver, due to its suitability and speed[5], in COMSOL's predefined Schrödinger equation and eigenvalue modes.

All calculations were done on 8-cores of the Brown Chemistry Department's UNIX Supercomputer with 4 GB of RAM.

5. Numerical Models

For the calculation of Trimethylamine (TMA) eigenvalues we used two GAUSSIAN cubes, one spanning from -50 bohr to 50 bohr in all directions, with a resolution of one evaluated electric potential point per bohr in each Cartesian direction and the other with an algorithmically optimized "normal" cube that spanned from -8.666 to 8.666 , -8.75 to 8.75, and -6.5 to 6.5 bohr with 6 points per bohr resolution. The geometry [fig. 1] is such that the inner cube has the dimensions of the second cube above and implements that cube's V while the rest of the spherical box implements that of the first GAUSSIAN potential cube, not utilizing all the potential points that lie outside its boundary. We then meshed the system under "normal" settings and set the inner cube's mesh element growth rate to 1 and that of the outer sphere to 50. We then solved, using the adaptive solver on default settings for 20 eigenvalues around -0.09 a.u., yielding only a few negative eigenvalues, of which we selected the wavefunction whose eigenvalue was closest to the experimental and computational values[6] and stored it as the initial condition of the system. This wavefunction was then mismatched with the -0.09 eigenvalue and a new batch of eigenvalues was returned. This process was repeated iteratively in the hope of getting solutions reminiscent of the expected eigenvalues and orbital character. We utilized quadratic Lagrange quadrature, as it was the highest order supported by the adaptive solver.

The GAUSSIAN calculations were at the B3LYP 6-311+** level and the molecular geometry was taken from microwave data,[7] as this configuration lead to the DFT results closest to experiment for the low lying Rydberg states calculated.[6]

The true hydrogen potential, evaluated analytically, and as an interpolated function on the same grid as TMA using a MATLAB script, was also run on the same solver and mesh settings, to provide a standard via which to examine the numerical accuracy of the model. The analytic potential was a point charge at the origin. We avoided the singularity there, in the grid case, by extending the TMA grids so they had an even number of entries in each direction.

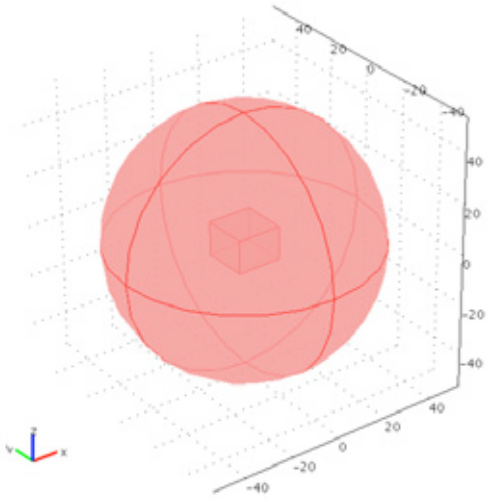

Figure 1. The geometry over which TMA eigenvalues were calculated; inner block measures (17, 17, 13), and the sphere is of radius 50.

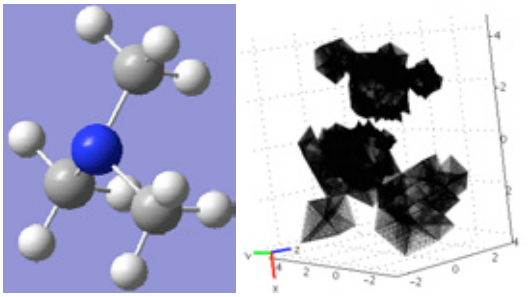

Figure 2. TMA molecular geometry: [Left] (GAUSSIAN): blue is nitrogen, gray is carbon, and white is hydrogen. [Right] (COMSOL) Plotting the 4.8% greatest values of ***V*** yields a visualization of the nuclear coordinates.

5. Results and Discussion

5.1 Hydrogen-like Orbital and Wavefunction

The wavefunctions associated with Hydrogen are used to describe Rydberg orbitals. Those in the range of energies probed are 3s and 3p, with the distinctions based on ℓ, the number of angular nodes. An s orbital is an orbital with spherical symmetry (no angular node). A p orbital has one angular node and higher order orbitals than these follow the alphabet and increase in the number of angular nodes (d, f, g, h). The number of radial nodes is 2-ℓ. Visualizing the wavefunction allows easy check of experimental assignment.

5.2 The Trimethylamine 3s Orbital

The 3s eigenvalue we calculated was -0.1221 a.u., falling within 7.6% of the experimental and within 3.7% of the theoretical values (-0.1134, -0.1176).[6] The value of $\sqrt{\langle r^2 \rangle}$ for this state is 3.917 bohr. This wavefuction can be visualized [fig. 3] and assigned [fig. 4] using COMSOL.

The $\sqrt{\langle r^2 \rangle}$ value tells us that our wave function lies about half outside of the molecular core [fig. 2]. Its general proximity to said core and lack of node at the origin probably contributes to its relatively high percent error.

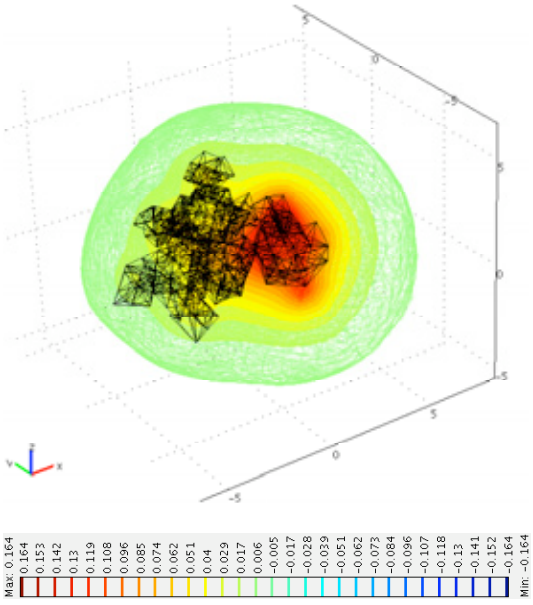

Figure 3. The normalized 3s wavefunction of TMA, plotted using 30 isosurfaces. The square of the value of the wavefunction is the probability density for the electron to be found at one of the elements on that level. This wavefunction has spherical symmetry outside of the core and, accordingly, s-like character.

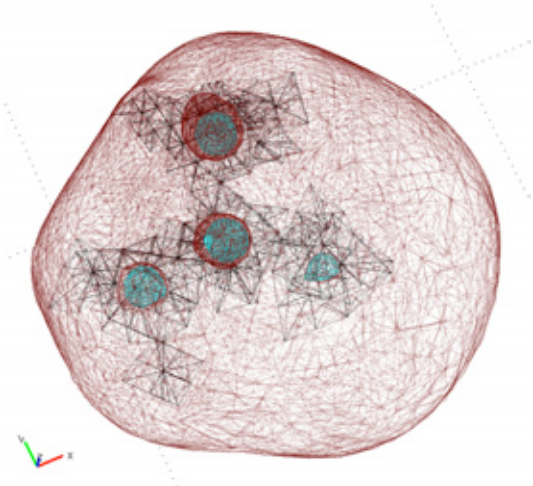

Figure 4. The 3s wavefunction of TMA. Two isosurfaces are plotted, corresponding to the wavefunction value ±.01. Red is positive, blue is negative. We can see two spherical nodes: one on the nitrogen, and another round of nodes on the carbon atoms.

5.3 The Trimethylamine 3p Orbital

The 3p eigenvalue was -0.0815 a.u. falling within 1.5% of the experimental $3p_{x,y}$ and 0.6% of the $3p_z$ and within 11.9% and 6.4% of their respective theoretical values (-0.0827, -0.0810, -0.0925, -0.08713).[6] Those theoretical values were within 10.6% and 7.0% of their associated experimental value, and as such, this eigenvalue represents the TMA 3p state [fig. 5] with greatest agreement with experiment yet calculated. $\sqrt{\langle r^2 \rangle}$ for this state is 4.038 bohr.

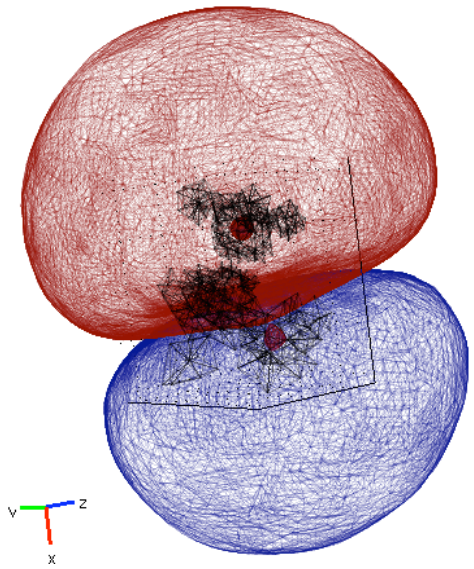

Figure 5. The 3p wavefunction TMA. Two isosurfaces are plotted, corresponding to the normalized wavefunction value ±.01. Red is positive. Note the nodal structure (both one spherical and one planar node) and that it is a $3p_x$ state as it lies along the x-axis. The axes are the same lengths as [fig. 2].

This $\sqrt{\langle r^2 \rangle}$ value tells us our wavefunction also lies about half outside of the molecular core [fig. 2] but its node at the origin probably leads to its increased accuracy. It also appears that, looking at the percent errors, our p_x state is closer to the assigned $3p_z$ state and thus casts some doubt on the assignment of the lower energy state to the $3p_z$.

5.4 Hydrogen Atom Baseline

The analytical hydrogen [fig. 6] data points to a very low solver inaccuracy. Eigenvalues 15 to 20 increased in error as a boundary artifact, as they are diffuse states in a 50 bohr spherical box. The low lying p and d states have almost no error and the error in 2s and 3s probably stem from their lower $\sqrt{\langle r^2 \rangle}$ and tendency toward a high field region, where numerical integration errors are compounded. The node of the p and d states at the origin probably contributes to their lower error, as well. The incredibly low error for the 14th 4s -0.03124 a.u. eigenvalue is because that is the first s state to rest firmly outside of the core, as its $\sqrt{\langle r^2 \rangle}$ value of 25.144 bohr avoids the singularity at the center, but is not diffuse enough to strongly feel the edge effects.

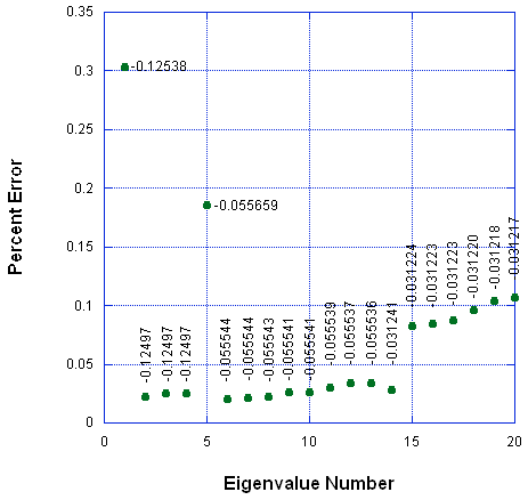

Figure 7. Analytic hydrogen solutions using the TMA solver and mesh settings. Eigenvalue 1 is the 2s, 2-4 are 2p, 5 is the 3s, 6-10 are 3d,11-13 are 3p, 14 is 4s, 15-17 are 4f and 18-10 are 4d. The data points are labeled with their eigenvalues.

The interpolated hydrogen [fig. 8] data shows the level of total error associated with the mesh, grid, and solver. Including the grid in these calculations appears to increase the error by only about an order of magnitude. The reason the order of s, p, d, and f states are now inverted is probably because of the artificial truncation of the singularity at the origin. The maximum ***V*** value for this run was 6.928 a.u., and this lack of dominant potential at the origin provides impetus for more diffuse wavefunctions.

It should also be noted that, in hydrogen, the higher the excited state the greater the accuracy. Our method of computing has exactly the opposite scaling effects as conventional *ab initio* calculation techniques.

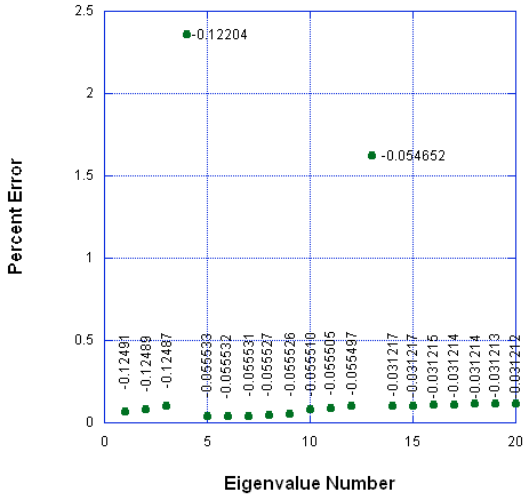

Figure 8. Interpolated hydrogen solutions using the TMA solver and mesh settings. Eignvalue 1-3 are 2p, 4 is the 2s, 5-9 is the 3d, 10-12 are 3p, 13 is 3s, 14-19 are 4f, and 20 is 4d. The data points are labeled with their eigenvalue.

6. Conclusion

Further analysis of the error; further improvement of solver, grid, and mesh settings; and a more effective algorithm to calculate bound (negative) eigenvalues are still needed before this becomes an optimal method for the calculation of Rydberg states. Regardless, the calculations show great promise and have provided accurate Trimethylamine eigenvalues. Further calculations should be done for Trimethylamine: both exploratory for new eigenvalues and as an analysis of the effects of different molecular core basis sets towards the accuracy of this general method. Besides these general improvements, this is a completely extendable method and could be utilized to probe the eigenvalues associated with the Rydberg states of any and all molecules of interest.

7. References

1. M. S. Child, *Molecular Rydberg Dynamics*, 1-15. Imperial College Press, London, UK (1999)
2. B. G. Johnson et. al "Computing Molecular Electrostatic Potentials with the PRISM Algorithm," Chem. Phys. Lett., **206**, 239-46 (1993)
3. M. J. Frisch et. al., *Gaussian 03, revision E01*; Gaussian Inc, Wallingford, CT, (2004)
4. *MATLAB 6.5.1*. Natick, Massachusetts: The MathWorks Inc., (2003)
5. N.I.M Gould et. al., "A numerical evaluation of sparse direct solvers for the solution of large sparse, symmetric linear systems of equations", *Rutherford Appleton Laboratory Technical Reports*, **5**, 1-35 (2005)
6. J.D. Cordoza et al, "Electronic Spectroscopy and Ultrafast Energy Relaxation Pathways in the Lowest Rydberg State of Trimethylamine", *J. Phys. Chem. A*, **112**, 10736-10743 (2008)
7. D. Lide, D.E. Mann, "Microwave Spectra of Molecules Exhibiting Internal Rotation III. Trimethylamine", *J. Chem. Phys.*, **28,** 572-6 (1958)

9. Acknowledgements

This project is supported by the Division of Chemical Sciences, Geosciences, and Biosciences, the Office of Basic Energy Sciences, the U.S. Department of Energy by grant number DE-FG02-03ER15452, and by the Army Research Office, Grant # W911NF-06-1-0463. We would like to thank Margaret Doll for making the computers work and Sanghimitra Deb, Joseph Bush, Xiao Liang, and Joseph Levy for their patience and enthusiasm in the context of these calculations.